THE JOURNAL OF PHYSICAL CHEMISTRY Letters

pubs.acs.org/JPCL

Collision Complex Lifetimes in the Reaction $C_6H_5 + O_2 \rightarrow C_6H_5O + O$

Daniel R. Albert and H. Floyd Davis*

Department of Chemistry and Chemical Biology, Baker Laboratory, Cornell University, Ithaca, New York 14853

ABSTRACT Phenyl radicals (C_6H_5) react with oxygen molecules (O_2) to form phenylperoxy radicals (C_6H_5OO). These intermediates have been calculated to decompose either through O−O bond fission forming $C_6H_5O + O$ or through a series of isomerization steps producing $C_5H_5 + CO_2$, $C_5H_5O + CO$, or $C_6H_4O_2 + H$. In this study, the reaction of phenyl radicals with molecular oxygen is investigated at a mean collision energy of 64 kJ/mol using the crossed molecular beams technique, employing detection via pulsed single-photon ionization at 9.9 eV. Here, we monitor the formation of phenoxy radicals (C_6H_5O) from the $C_6H_5O + O$ channel, providing insight into the lifetimes of the C_6H_5OO intermediates. The measured distributions imply that the C_6H_5OO lifetimes (τ) are at least comparable to their rotational time scales, that is, $\tau \geq 1$ ps. Our lower limit for τ is at least 100 times longer than an upper limit inferred from a previous crossed beams experiment carried out at a higher energy.

SECTION Dynamics, Clusters, Excited States

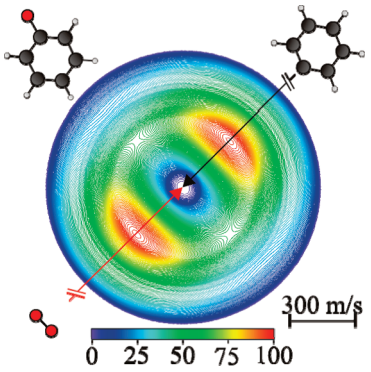

The phenyl radical (C_6H_5) is an important intermediate in combustion, playing a significant role in the oxidation of aromatic species and in soot buildup, where the formation and then subsequent reaction of the first aromatic ring is a key step.[1−3] The reaction of C_6H_5 with O_2 can compete directly with other addition processes, that is, addition of phenyl to unsaturated hydrocarbons, leading to the formation of polycyclic aromatic hydrocarbons (PAHs). The products from reaction of phenyl radicals with molecular oxygen could lead to a suppression of PAHs or to the formation of new PAH building blocks, namely, cyclopentadienyl radicals (C_5H_5).[1,2] Since PAHs are thought to be soot precursors, understanding the oxidation of C_6H_5 is critical to modeling the evolution of soot particles.[1−3] Much work has been done, both theoretically[4−7] and experimentally,[8−13] to understand the mechanism of phenyl oxidation.

Electronic structure calculations have focused on the potential energy surfaces for reaction, with particular focus on the structure and energetics of the key reaction intermediates. From theoretical calculations, the $C_6H_5 + O_2$ reaction is expected to proceed via addition without a potential energy barrier to form phenylperoxy radicals (C_6H_5OO) bound by 194 kJ/mol relative to the reactants.[6] These intermediates can become stabilized by subsequent collisions[10] or can decompose to a variety of products (Figure 1). In high-temperature shock tube studies by Frank et al., the production of H, O, and CO was detected, leading to the prediction of two product channels, $C_6H_5O + O$ and $C_6H_4O_2 + H$. The C_6H_5O was thought to then decompose to C_5H_5 and CO.[9] Recently, the reaction was studied in a crossed molecular beams apparatus by Gu and co-workers. The only observed reaction involved formation of $C_6H_5O + O$.[13]

Calculations indicate that the O−O bond fission channel should produce $C_6H_5O + O$ with no potential energy barrier above the reaction endoergicity.[6] The other energetically accessible channels, although more exothermic, require multiple isomerization steps.[6] The lifetime of the C_6H_5OO intermediate (τ) is the inverse of the sum of the rate constants (k) for all competing C_6H_5OO decomposition pathways. In the previous crossed molecular beams study using a pyrolytic phenyl radical source at a nominal collision energy of ~107 kJ/mol, the $C_6H_5O + O$ channel was found to proceed through a direct mechanism with decomposition lifetimes of any C_6H_5OO intermediates shorter than 0.01 ps.[13] A rate constant for O−O bond fission greater than 10^{14} s^{-1} would effectively close all competing reaction pathways as they involve multiple isomerization steps via "tight" transition states.[6] Here, we have examined the reaction using a photolytic source of phenyl radicals at a lower collision energy using a newly developed pulsed 9.9 eV vacuum ultraviolet (VUV) photoionization method. The dynamics inferred from our study are quite different from those inferred from the previous work.

Crossed molecular beams experiments were performed with a rotatable sources machine,[14] where the phenyl radical beam intersected a pulsed beam of O_2 at a right angle, leading to a mean collision energy of 64 kJ/mol. Products traveled 24.1 cm before being ionized by 9.9 eV photons, mass filtered, and detected as a function of arrival time. Time-of-flight (TOF) spectra were recorded at various laboratory

Received Date: February 12, 2010
Accepted Date: March 10, 2010
Published on Web Date: March 15, 2010

DOI: 10.1021/jz100199z | *J. Phys. Chem. Lett.* **2010**, *1*, 1107–1111

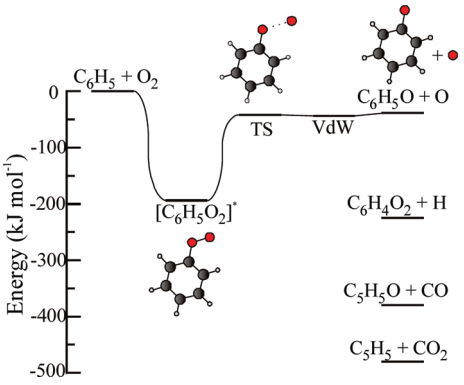

Figure 1. Simplified potential energy diagram for the $C_6H_5 + O_2 \rightarrow C_6H_5O + O$ reaction, where TS is the transition state for O−O bond fission and VdW is the van der Waals complex between the phenoxy radical and oxygen atom. Overall energetics for other major reaction channels predicted by Tokmakov et al. are shown. Adapted from ref 6.

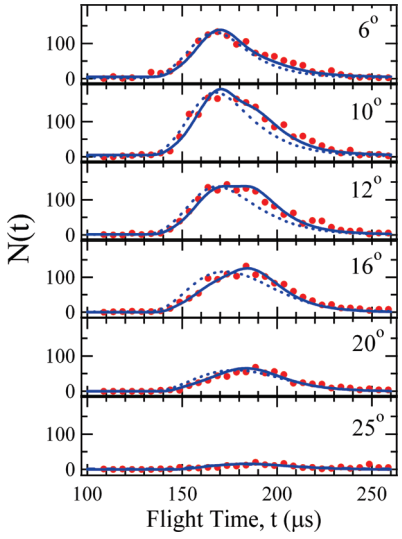

Figure 2. Measured TOF spectra obtained at various laboratory angles for $C_6H_5O^+$ (m/e = 93) products. Solid dots are experimental data; solid lines are calculated using optimized center-of-mass translational energy and angular distributions (Figure 4); dotted lines show fits using an osculating complex angular distribution.

angles for m/e = 93, $C_6H_5O^+$. Each TOF spectrum, shown as solid dots in Figure 2, consisted of ∼30 000 laser shots, corresponding to ∼20 min of data collection time. At angles close to the phenyl beam, a small amount of time-dependent background signal was present. By carrying out parallel studies in which a N_2/He mixture was used instead of an O_2/He mixture, this signal was found to result from nonreactive scattering of minor impurities in the phenyl beam. This signal was therefore subtracted out from each TOF spectrum.

The laboratory angular distribution was constructed by integrating each TOF spectrum, as indicated by solid dots in Figure 3. The lines in Figures 2 and 3 are simulations of the experimental data calculated using the forward convolution technique described previously.[15] Briefly, a computer program took as inputs a center-of-mass (CM) translational energy distribution, $P(E)$, and a CM angular distribution, $T(\theta)$,

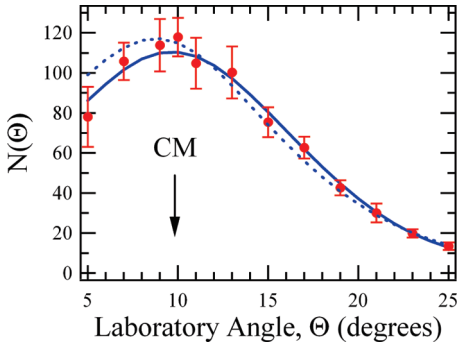

Figure 3. Laboratory angular distribution for C_6H_5O products. Solid dots are experimental data with 1σ error bars. The solid line is calculated using optimized center-of-mass distributions from Figure 4, and the dotted line is calculated using an osculating complex $T(\theta)$, also shown in Figure 4. CM denotes the angle of the center-of-mass.

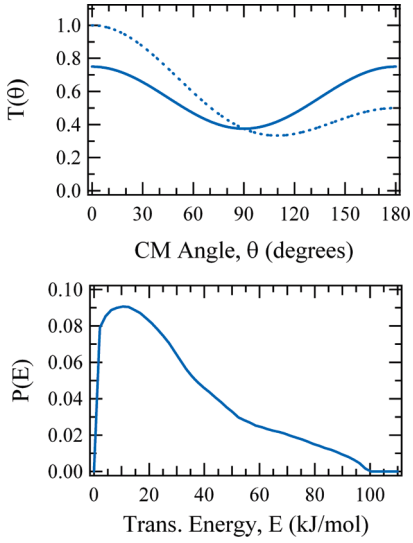

Figure 4. Solid lines: Optimized C_6H_5O center-of-mass angular distribution, $T(\theta)$, and translational energy distribution, $P(E)$. Dotted line: Osculating complex $T(\theta)$.

along with known instrument and beam parameters and calculated TOF spectra and laboratory angular distributions. The two input functions were then iteratively adjusted until agreement was reached between the experimental and calculated distributions. The optimized $P(E)$ and $T(\theta)$ for the $C_6H_5O + O$ channel are shown as solid lines in Figure 4.

We find that the $P(E)$ peaks at low translational energy release ∼12 kJ/mol. This is characteristic of a reaction in which no significant potential energy barrier exists for O−O bond fission in C_6H_5OO above its endoergicity, that is, the maximum in the potential energy along the reaction pathway is primarily due to the centrifugal barrier, corresponding to decay via a "loose" transition state. This is consistent with calculations that predict no significant exit barrier for C_6H_5OO decomposition to $C_6H_5O + O$.[6,7]

The optimized center-of-mass angular distribution is forward−backward-symmetric (Figure 4, solid line). A forward−backward-symmetric angular distribution is characteristic of a

DOI: 10.1021/jz100199z | J. Phys. Chem. Lett. 2010, 1, 1107–1111

reaction involving C_6H_5OO collision complexes with lifetimes of at least several rotational periods. The shortest rotational times available to phenylperoxy intermediates, while still conserving orbital angular momentum, are 0.5, 1.7, and 2.2 ps. For reactions involving "osculating complexes", that is, collision complexes having lifetimes comparable to their rotational periods, a more forward-peaking CM angular distribution is often observed, as indicated by the dotted line in Figure 4.[16,17] In Figures 2 and 3, we include the calculated laboratory angular and TOF distributions as dotted lines, assuming decomposition of an osculating complex with a CM angular distribution shown as a dotted line in Figure 4. These calculated distributions do not simulate the experimental data as well as when a fully forward−backward-symmetric distribution is employed, indicating that the C_6H_5OO lifetimes are not likely to be as short as one rotational period.

Our conclusion that the reaction is dominated by formation of long-lived collision complexes followed by simple O−O bond fission at a mean collision energy of 64 kJ/mol is significantly different from that of Gu et al.[13] They concluded that the reaction proceeded via a direct mechanism near the spectator stripping limit, imposing a maximum C_6H_5OO lifetime of ∼0.01 ps. This time scale is at least 2 orders of magnitude shorter than the lower limit inferred from our work. To better appreciate the large difference between our results, we have calculated the laboratory angular and TOF distributions using a $P(E)$ and $T(\theta)$ similar to those presented in ref 13. These calculated distributions, available as Supporting Information, differ markedly from our experimental measurements.

While both studies were carried out using the method of crossed beams employing pulsed sources for each beam, there are considerable experimental differences. Most notably, the C_6H_5 reactants were produced in our study by photodissociation of C_6H_5Cl in a room-temperature nozzle, whereas in their work, the C_6H_5 was produced by flash pyrolysis of C_6H_5NO at ∼1350 K.[13,18] In addition, our experiment was carried out at a lower mean collision energy.

Could the sharply differing dynamics reported in the only two existing crossed beam studies of $C_6H_5 + O_2$ be attributable to the different experimental conditions? Beams of polyatomic free radicals have been produced with a variety of different ways including chemical reaction,[19] electrical discharge,[20] pyrolysis,[21] and photolysis.[22] To date, there has been relatively little attention paid to how preparation of radicals can affect their reaction dynamics. In the future, we plan to compare the dynamics of the $C_6H_5 + O_2$ reaction using both photolytic and pyrolytic sources of C_6H_5 as a function of collision energy, with all other experimental conditions the same. Until such experiments can be carried out, Rice−Ramsperger−Kassel−Marcus (RRKM) calculations,[23] performed with a standard program,[24] can provide some insight into how the different experimental conditions might affect the measurements.

In pyrolysis sources, precursors are passed through a hot (up to 2000K) SiC tube, causing decomposition into the corresponding radicals and byproducts.[21] While this approach can produce rather intense radical beams, secondary reactions within the tube, where temperatures and pressures are high, can lead to impurities. Furthermore, the level of vibrational excitation can be large since vibrational energy is not as effectively cooled as rotations upon supersonic expansion.[25] Here, we assume that the vibrational temperature of the phenyl radicals employed in ref 13 is equal to the nozzle temperature, reported to be T = 1350 K.[18] Assuming a statistical vibrational distribution and approximating the vibrational modes as independent harmonic oscillators with the vibrational frequencies of C_6H_5,[26] we calculate the average energy in each vibrational mode utilizing the vibrational partition function. The average total vibrational energy at 1350 K is the sum of the individual average energies, yielding 148 kJ/mol for C_6H_5 produced by pyrolysis of C_6H_5NO.

In our photolytic source, a laser is used to photodissociate C_6H_5Cl, and the internal energy distributions of the radicals are governed by the photodissociation dynamics. Chlorobenzene photodissociation at 193 nm has been well-characterized by Sveum et al. using VUV photoionization detection of the products employing a synchrotron light source.[27] It is known that three distinct channels exist. By integrating the areas of the published $P(E)$ distributions, the branching ratio for the three channels is 55:42:3. Using the mean translational energy release for each channel, the average excess energy for the $C_6H_5 + Cl$ products is ∼130 kJ/mol. Since the spin−orbit splitting in Cl atoms is only 10.6 kJ/mol, most of the excess available energy is C_6H_5 vibrational energy. Assuming no vibrational cooling during the expansion and ignoring the energy deposited into spin−orbit-excited Cl, the C_6H_5 radicals produced by photolysis in our experiment have, on average, about 88% as much vibrational energy as those produced by pyrolysis in the work of Gu et al.[13]

The mean collision energy employed in our study (64 kJ/mol) is smaller than that in the previous study (107 kJ/mol). This factor will also produce a greater level of excitation in any C_6H_5OO complexes formed in the reaction in the work of Gu, leading to shorter lifetimes in their experiment. Using the mean C_6H_5 vibrational energies, mean collision energies, and $D_o(C_6H_5-O_2)$ = 194 kJ/mol, the mean total vibrational energy, E, of the C_6H_5OO complexes is 388 kJ/mol in our experiment and 449 kJ/mol in the work of Gu et al. The minimum energy for reaction, E_o, is calculated to be $D_o(C_6H_5O-O)$ = 152 kJ/mol.[6]

Assuming that RRKM theory is applicable to the C_6H_5OO intermediates, which have 13 atoms and 33 vibrational degrees of freedom, our calculations should provide at least an order of magnitude estimate of decay rates. Using the vibrational frequencies and moments of inertia from ref 6, together with the values of E and E_o given above, we calculated RRKM rate constants, k_{uni}, for unimolecular decomposition of C_6H_5OO to $C_6H_5O + O$. The mean lifetimes τ (= $1/k_{uni}$) were calculated to be $\tau \approx 260$ ps for E = 388 kJ/mol and $\tau \approx 70$ ps for E = 449 kJ/mol. These RRKM lifetimes correspond to many C_6H_5OO rotational periods, consistent with a forward−backward-symmetric angular distribution. The spectator stripping dynamics reported in ref 13 implies C_6H_5OO lifetimes almost 4 orders of magnitude smaller than our RRKM calculations. They are at least 2 orders of magnitude shorter than the lower limit inferred from our experiments

DOI: 10.1021/jz100199z | J. Phys. Chem. Lett. 2010, 1, 1107–1111

carried out at a lower collision energy using a colder phenyl radical beam.

In future studies, we plan to examine how C_6H_5OO lifetimes depend upon experimental parameters such as the source of C_6H_5 (i.e., internal energy) and the reactant collision energy. Our results, together with RRKM calculations, suggest that the isomerization pathways producing other products may compete with the $C_6H_5O + O$ channel. This will be examined in future studies employing VUV ionization wavelengths appropriate for detecting the other channels.

EXPERIMENTAL METHODS

The experiments were carried out using a rotatable source, fixed detector crossed molecular beams apparatus.[14] The phenyl beam was produced by the photodissociation of chlorobenzene (~10 Torr) using a pulsed excimer laser (Lambda Physik LPX 210i) operating at 193 nm. The output of the excimer laser was spatially filtered by a macor aperture and gently focused to a 6 mm × 2 mm spot directly in front of the orifice of the pulsed valve. The phenyl beam ($\langle v \rangle$ = 2180 ms^{-1}, speed ratio = 10), seeded in 20 PSIG of H_2 carrier gas, passed through a 2.0 mm diameter skimmer (Beam Dynamics) into the main chamber region, maintained at or below ~5×10^{-6} Torr. The O_2 beam was generated by the supersonic expansion of a 40 % O_2 in He mixture operating at 40 PSIG ($\langle v \rangle$ = 950 ms^{-1}, speed ratio = 12). This beam is collimated by a 2.0 mm diameter skimmer (Precision Instruments) before entering the main chamber and crossing the phenyl beam at a 90°collision angle. The O_2 beam was characterized in a separate series of experiments by monitoring its TOF distributions on-axis using a slotted chopper wheel with a mass spectrometer detector employing electron impact ionization detection. Scattered species traveled 24.1 cm through a series of three apertures and were ionized in a region maintained below 1×10^{-10} Torr by a single VUV photon at ~9.9 eV. The resulting positive ions were mass selected using a quadrupole mass filter (Extrel Merlin with 0.75 in. rods) and were detected using a conversion dynode/electron multiplier operating in pulse counting mode.

The pulsed VUV light was generated by resonance-enhanced four wave mixing in mercury vapor using two collimated (unfocused; ~2 mm diameter) laser beams via the two-photon resonance at 312.8 nm and a third photon near 622 nm.[28,29] The 312.8 nm light was generated by frequency doubling the output of a nanosecond Nd:YAG (Continuum 9030 with injection seeder) pumped dye laser (Scanmate 2), while the 622 nm light came directly from a second dye laser (Scanmate 2). The dye lasers were aligned spatially and temporally through a 1 m long mercury heat pipe at ~400 K. The wavelength of the 622 nm laser was tuned to maximize the VUV intensity by index matching just to the red of the 9 ^1P state at 79 964 cm^{-1}.[28] A slow flow of helium buffer gas directed away from the windows at approximately 50 Torr of total pressure protected the optics at each end of the cell from contamination. The VUV beam was spatially dispersed from the UV and visible beams by transmission off-axis through a 50 cm focal length MgF_2 lens (ISP Optics). The VUV passed by the edge of a macor beam dump mounted on a linear translation stage, while the UV and visible beams (dispersed through a smaller angle than the VUV) were dumped before arriving in the ionization region of the detector.

The TOF arrival distributions were generated by scanning the delay of the ionization laser relative to the excimer laser. By rotating the source assembly relative to the detector and measuring the TOF spectra at separate laboratory angles with respect to the phenyl molecular beam axis, the laboratory angular and kinetic energy distributions were determined.

SUPPORTING INFORMATION AVAILABLE Experimental laboratory angular distribution and TOF spectra, showing simulations using $P(E)$ and $T(\theta)$ similar to those in ref 13. This material is available free of charge via the Internet at http://pubs.acs.org.

AUTHOR INFORMATION

Corresponding Author:

*To whom correspondence should be addressed. E-mail: hfd1@cornell.edu.

ACKNOWLEDGMENT The authors would like to thank David Proctor for his work in helping to develop the VUV source employed in this work and Alexander Mebel (Florida International University) for helpful discussions pertaining to the RRKM calculations. This research was supported by the National Science Foundation under Grant CHE-0809622 and by the Office of Science, U.S. Department of Energy, under Grant DE-FG02-00ER15095.

REFERENCES

(1) Miller, J. A.; Pilling, M. J.; Troe, J. Unraveling Combustion Mechanisms Through a Quantitative Understanding of Elementary Reactions. *Proc. Combust. Inst.* **2005,** *30*, 43–88.
(2) Frenklach, M. Reaction Mechanism of Soot Formation in Flames. *Phys. Chem. Chem. Phys.* **2002,** *4*, 2028–2037.
(3) Glassman, I. *Combustion*; Academic Press: Orlando, FL,1987.
(4) Carpenter, B. Computational Prediction of New Mechanisms for the Reactions of Vinyl and Phenyl Radicals with Molecular-Oxygen. *J. Am. Chem. Soc.* **1993,** *115*, 9806–9807.
(5) Barckholtz, C.; Fadden, M. J.; Hadad, C. M. Computational Study of the Mechanisms for the Reaction of O_2 ($^3\Sigma_g$) with Aromatic Radicals. *J. Phys. Chem. A* **1999,** *103*, 8108–8117.
(6) Tokmakov, I. V.; Kim, G. S.; Kislov, V. V.; Mebel, A. M.; Lin, M. C. The Reaction of Phenyl Radical with Molecular Oxygen: A G2M Study of the Potential Energy Surface. *J. Phys. Chem. A* **2005,** *109*, 6114–6127.
(7) da Silva, G.; Bozzelli, J. W. Variational Analysis of the Phenyl + O_2 and Phenoxy + O Reactions. *J. Phys. Chem. A* **2008,** *112*, 3566–3575.
(8) Sommeling, P. M.; Mulder, P.; Louw, R.; Avila, D. V.; Lusztyk, J.; Ingold, K. U. Rate of Reaction of Phenyl Radicals with Oxygen in Solution and in the Gas Phase. *J. Phys. Chem.* **1993,** *97*, 8361–8364.
(9) Frank, P.; Herzler, J.; Just, T. H.; Wahl, C. High-Temperature Reactions of Phenyl Oxidation. *Twenty-Fifth Symposium on Combustion* **1994,** 833–840.
(10) Yu, T.; Lin, M. C. Kinetics of the $C_6H_5 + O_2$ Reaction at Low Temperatures. *J. Am. Chem. Soc.* **1994,** *116*, 9571–9576.
(11) Schaugg, J.; Tranter, R. S.; Grotheer, H. H. In *Transport Phenomena in Combustion*; Chan, S. H., Ed.; Taylor and Francis: Washington DC, 1996; Vol. 1, pp130−141.

DOI: 10.1021/jz100199z | *J. Phys. Chem. Lett.* **2010,** *1*, 1107–1111

(12) Tonokura, K.; Norikane, Y.; Koshi, M.; Nakano, Y.; Nakamichi, S.; Goto, M.; Hashimoto, S.; Kawasaki, M.; Sulbaek Anderson, M. P.; Hurley, M. D.; Wallington, T. J. Cavity Ring-Down Study of the Visible Absorption Spectrum of the Phenyl Radical and Kinetics of its Reactions with Cl, Br, Cl_2 and O_2. *J. Phys. Chem. A* **2002,** *106*, 5908–5917.
(13) Gu, X.; Zhang, F.; Kaiser, R. I. Crossed Beam Reaction of the Phenyl Radical, (C_6H_5, X_2A') with Molecular Oxygen (O_2, ($X^3\Sigma g$): Observation of the Phenoxy Radical, (C_6H_5O, X_2A'). *Chem. Phys. Lett.* **2007,** *448*, 7–10.
(14) Willis, P. A.; Stauffer, H. U.; Hinrichs, R. Z.; Davis, H. F. Rotatable Source Crossed Molecular Beams Apparatus with Pulsed Vacuum Ultraviolet Photoionization Detection. *Rev. Sci. Instrum.* **1999,** *70*, 2606–2614.
(15) Willis, P. A.; Stauffer, H. U.; Hinrichs, R. Z.; Davis, H. F. Reaction Dynamics of Zr and Nb with Ethylene. *J. Phys. Chem. A.* **1999,** *103*, 3706–3720.
(16) Fisk, G. A.; McDonald, J. D.; Herschbach, D. R. General Discussion. *Faraday Discuss. Chem. Soc.* **1967,** *44*, 228–229.
(17) Alagia, M.; Balucani, N.; Casavecchia, P.; Stranges, D.; Volpi, G. G. Crossed Beam Studies of Four-Atom Reactions: The Dynamics of OH + CO. *J. Chem. Phys.* **1993,** *98*, 8341–8344.
(18) Gu, X.; Kaiser, R. I. Reaction Dynamics of Phenyl Radicals in Extreme Environments: A Crossed Molecular Beam Study. *Acc. Chem. Res.* **1987,** *42*, 290–302.
(19) Kaiser, R. I.; Ting, J. W.; Huang, L. S.; Balucani, N.; Asvany, O.; Lee, Y. T.; Chan, H.; Stranges, D.; Gee, D. A Versatile Source to Produce High-intensity, Pulsed Supersonic Radical Beams for Crossed-Beam Experiments: The Cyanogen Radical CN-($X^2\Sigma^+$) as a Case Study. *Rev. Sci. Instrum.* **1999,** *70*, 4185–4191.
(20) Dong, F.; Roberts, M.; Nesbitt, D. J. High Resolution Infrared Spectroscopy of Jet Cooled Vinyl Radical: Symmetric CH_2 Stretch Excitation and Tunneling Dynamics. *J. Chem. Phys.* **2008,** *128*, 044305.
(21) Kohn, D. W.; Clauberg, H.; Chen, P. Flash Pyrolysis Nozzle for Generation of Radicals in a Supersonic Jet Expansion. *Rev. Sci. Instrum.* **1992,** *63*, 4003–4005.
(22) Davis, H. F.; Shu, J.; Peterka, D. S.; Ahmed, M. Crossed Beams Study of the Reaction $^1CH_2 + C_2H_2 \rightarrow C_3H_3 + H$. *J. Chem. Phys.* **2004,** *121*, 6254–6257.
(23) Baer, T.; Hase, W. L. *Unimolecular Reaction Dynamics*; Oxford University Press: New York, 1996.
(24) Zhu, L.; Hase, W. L. *Program 644, Quantum Chemistry Program Exchange*; Indiana University: Bloomington, IN, 1994.
(25) Miller, D. R. In *Atomic and Molecular Beam Methods*; Scoles, G., Ed.; Oxford University Press: New York, 1988; Vol. 1, p 35.
(26) Friderichsen, A. V.; Radziszewski, J. G.; Nimlos, M. R.; Winter, P. R.; Dayton, D. C.; David, D. E.; Ellison, G. B. The Infrared Spectrum of the Matrix-Isolated Phenyl Radical. *J. Am. Chem. Soc.* **2001,** *123*, 1977–1988.
(27) Sveum, N. E.; Goncher, S. J.; Neumark, D. M. Determination of Absolute Photoionization Cross Sections of the Phenyl Radical. *Phys. Chem. Chem. Phys.* **2006,** *8*, 592–598.
(28) Smith, A. V.; Alford, W. J. Practical Guide for 7S Resonant-Frequency Mixing in Mercury-Generation of Light in the 230−185 and 140−120 nm Ranges. *J. Opt. Soc. Am. B* **1987,** *4*, 1765–1770.
(29) Hilbig, R.; Wallenstein, R. Resonant Sum and Difference Frequency Mixing in Hg. *IEEE J. Quant. Electron.* **1983,** *QE-19*, 1759–1770.

DOI: 10.1021/jz100199z | *J. Phys. Chem. Lett.* **2010,** *1*, 1107–1111